



# Investigating the materials used in eighteenth-century tapestries from the three French Royal Manufactories: inputs of hyperspectral approaches

Hortense De La Codre<sup>1,2,a</sup> , Floréal Daniel<sup>1</sup>, Rémy Chapoulié<sup>1</sup>, Laurent Servant<sup>2</sup>, Aurélie Mounier<sup>1</sup>

<sup>1</sup> IRAMAT-CRP2A- UMR 5060 CNRS, University Bordeaux Montaigne, Pessac, France

<sup>2</sup> Institut des Sciences Moléculaires- UMR 5255 CNRS, University of Bordeaux, Talence, France

Received: 6 May 2021 / Accepted: 15 November 2021

© The Author(s), under exclusive licence to Società Italiana di Fisica and Springer-Verlag GmbH Germany, part of Springer Nature 2021

**Abstract** At the end of the seventeenth century, three “Royal” tapestry Manufactories existed thanks to Louis XIV’s first minister, Jean-Baptiste Colbert: Aubusson, Gobelins and Beauvais. This newly acquired title gave rise to the establishment of numerous rules concerning the quality of the materials used for the production of tapestries. These quality standards were ensured by inspectors of the Crown and renowned cartoon painters sent to work in the Manufactories, which led to the birth of the so-called *Tapisseries de Grand Teint*. To facilitate the study of these high-quality tapestries, a colour chart consisting of more than 600 references based upon formulations from eighteenth-century treatises was created including spectra recorded with two hyperspectral cameras, in the visible–near infrared and short-wave infrared ranges. This reference database was then used in comparison with the spectra recorded in situ on the three tapestries included in the present study. Ultimately, this method allows for the identification of the specific materials used for tapestry fabrication. This paper presents the results of a comparative analysis of tapestries produced in each of the three Royal Manufactories through the use of two distinct and widely used approaches (i.e. through external and internal databases). The first approach relies upon comparisons with an external database via the Spectral Angle Mapper for the classification and mapping of the tapestry materials. The second method classifies the data by first extracting endmembers (reference spectra of pure materials) directly from the tapestry and then creating an internal database using the ENVI-Spectral Hourglass Wizard. This study emphasises the efficiency of each method as well as noting their limitations due to the specificities of the materials studied in the identification of tapestry textiles and dyes. The investigations revealed, for example, differences between the Manufactories in how different textiles were used in the production of tapestries. This comparison thus sheds light on the technical and aesthetic choices of the Manufactories and how they differ.

<sup>a</sup> e-mail: [hortense.de-la-codre@u-bordeaux-montaigne.fr](mailto:hortense.de-la-codre@u-bordeaux-montaigne.fr) (corresponding author)

## 1 Introduction

At the end of the seventeenth century, Louis XIV's first minister, Jean-Baptiste Colbert, reorganised the "Arts" in France to better compete with foreign nations. Among other things, he created several Royal tapestry production establishments that would receive support from the Crown. The Gobelins Manufactory was the first to benefit from this newfound support and saw the most talented artists, painters, and dyers come together. This was followed by the Beauvais Manufactory and finally the numerous Aubusson workshops. This new royal endorsement led to the implementation of strict rules concerning the quality of the materials used for the production of tapestries. To maintain the high royal standards, quality control was carried out by inspectors of the Crown and renowned cartoon painters sent to work in the Manufactories [1]. Among the regulations put in place was a list of authorised dyes, called *Grand Teint* dyes. These dyes were deemed strong enough to withstand the passage of time by the chemist of the Royal Academy of Sciences [2, 3] and produced fairly bright hues. In a somewhat schematic view, it is typically generalised that the Gobelins made tapestries for the King, Beauvais for the aristocracy, and Aubusson for foreign exportation. This perception must nevertheless be qualified, however, because the use of a particular tapestry was dependent upon the subject matter of its design. Moreover, Aubusson did, in fact, produce high quality tapestries in the eighteenth century, some of which can still be seen at the *Cité Internationale de la Tapisserie* in Aubusson, notably including those displaying the arms of the Polish-Saxon statesman, Count Heinrich von Brühl (Fig. 1).

Generally speaking, tapestries are composed of three main compounds: mordant, dye, and textile. The dyes were fixed to the substrate, in our case the fabric, with the help of mordants. These are metal salts that allow the formation of an organometallic complex between the dye and the textile to facilitate adhesion. In the eighteenth century, the fabrics authorised for the *Grand Teint* were dyed silk and wool yarns. These were woven around a warp yarn, generally of cotton, which would no longer be visible once the tapestry was completed. Formulations for *Grand Teint* dyeing used during this period were gathered from old treatises [2–8] and then recreated in a colour chart made of several hundred samples.



**Fig. 1** Tapestry (3,44 m × 7,32 m) with the arms of Count von Brühl from a cartoon by J-J. Dumons, Aubusson Manufactory, 1753. © Cyril Fressillon-CNRS Photothèque

These samples allowed for the subsequent recording of a spectral database with different non-invasive techniques, notably via hyperspectral imaging in the visible–near infrared (V-NIR) and short-wave infrared (SWIR) ranges. In the present study, the data from the tapestries were acquired under these same conditions to allow for a comparison, leading to the potential identification of the materials used.

Two cameras were used for the spectra acquisitions, one in the V-NIR (400–1000 nm) and the other in the SWIR range (1000–2500 nm). The visible range allows the identification of dyes or pigments via molecular absorption bands and has been previously used by many teams either with a hyperspectral camera or for point analysis with fibre optic reflectance spectroscopy (FORS) [9–12]. In a complementary way, the SWIR domain provides signatures of molecular vibrations [13, 14] that in our case appear specific to the particular textiles used in tapestries [15]. Hyperspectral imaging allows for the collection of a large amount of data from a single image. Thus, this technique provides the opportunity to map the materials used to produce an artwork by means of various classification methods. Indeed, while the relevance of each of these methods can be debated, they have each previously proven their effectiveness on certain materials. The method which uses an external database through the Spectral Angle Mapper (SAM) supervised classification works by associating an angle between each spectrum of the hyperspectral image and a reference spectrum from external samples. This method allowed Aurélie Mounier’s team [16] in 2014 and Floréal Daniel [17] in 2016 to successfully classify pigments of miniatures and paintings. John Delaney in 2010 [13] and later Tania Kleynhans [18] also discuss this classification method by comparing it with the internal database method. Through numerous steps, they extracted reference spectra data directly from the artwork through the “ENVI-Spectral Hourglass Wizard” (SHW) for utilisation as reference spectra for SAM classification. Though these two methods clearly have their advantages, they also feature limitations when identifying and mapping the material used in tapestries.

The following study compares the material choices in the production of three different tapestries, one from each of the three Royal Manufactories. Their comparison raises questions about the economic and artistic realities surrounding the Manufactories in the eighteenth century, as some dyes and textiles were undoubtedly more expensive than others. Therefore, the identification of the quantity of specific materials used to produce the tapestries from certain Manufactories makes it possible to place the producers and their products within a broader French and overall European context.

This study also highlights the differences between two hyperspectral imaging data cube classification systems (i.e. through internal versus external databases). Ultimately, the use of a classification system permits us to map some of the tapestry materials used in the eighteenth century and thus better understand differential production techniques in the French Manufactories. Furthermore, the detailed study of the materials is possible due to the complementarity of hyperspectral imaging in the V-NIR and SWIR domains.

The paper is organised as follows:

First, reference material and the tapestries studied will be introduced as well as the specifics of the two hyperspectral imaging cameras which were used for data collection. Following the materials and equipment descriptions, the two methods of data classification employed in this work, i.e. the external and the internal database, will be presented and discussed. The tools (SAM and SHW) used to map the data are also described below.

Our results are then presented in three parts. The “Textile identification” section details three methods used to map the textile composition: a simple “visualisation” method of the HSI image and then the two classification methods, respectively, based upon internal and external databases. Once the most relevant method to map the textile composition in the

SWIR range has been identified, we then apply it to the selected three artworks in order to discuss the type of textiles used in tapestry production. The identification and classification of the dyes in the tapestries are then addressed in terms of the madder colour chart using the external database method in the V-NIR range.

Finally, we discuss the application of this method for the analysis of tapestries through the example of one Aubusson tapestry and note the observations raised from such mapping.

## 2 Materials

### 2.1 Colour chart

The reference colour chart was constructed by selecting dyes from the *Grand Teint* for each colour formerly known as “primitives”: blue, red, yellow, tawny and black. Each dye was prepared according to eighteenth-century formulations [2–7, 19], but also through varying the proportions of the different compounds and mixing the dyes. This resulted in a colour chart of over 600 distinct samples. These comparative reference samples were dyed at the Myrobolan dye workshop in Brussels. In our analysis, we will then take one example from our analytical approach through the madder dye colour chart. Those formulations of madder on wool are described in Table 1.

The 600 samples of the colour chart were used to record reference spectra to constitute the external database. Moreover, these reference spectra give specific absorption bands for each dye. Thus, they allow for the attribution of absorption bands for the endmembers extracted from the tapestries (which constitute the internal database).

### 2.2 Archaeological materials

To facilitate a comparative study of the Aubusson Manufactory with the Gobelins and Beauvais Manufactories in the eighteenth century, one tapestry from each was selected according to several parameters. The Aubusson tapestry (Fig. 1) was made after a renowned cartoon painter, Jean-Joseph Dumons. It is thus essential to compare tapestries made after the most prestigious painter of Gobelins and Beauvais as well, namely François Boucher. With *Verdures* (vegetal designs) being a particular speciality of Aubusson, it was necessary to study subjects which likewise made the other two factories famous, but were also creations similar to the work of Aubusson. The choice fell on two tapestries (Fig. 2) representing mythological scenes, including some elements of *Verdures*.

**Table 1** Formulations of model samples (for 100 g of wool)

Sample number	Mordant	Dye (Madder)
01A	31 g alum; 6 g tartar; 12 g citric acid	50 g
01B to 01F	These samples were successively soaked for 45 min in the dye bath of sample 01A without adding more dye	
01 BIS PHy	31 g alum; 6 g tartar; x g citric acid*	100 g
02	31 g alum; 6 g tartar; 12 g citric acid	30 g

\*The citric acid mass was added until the desired pH was achieved in the dye bath

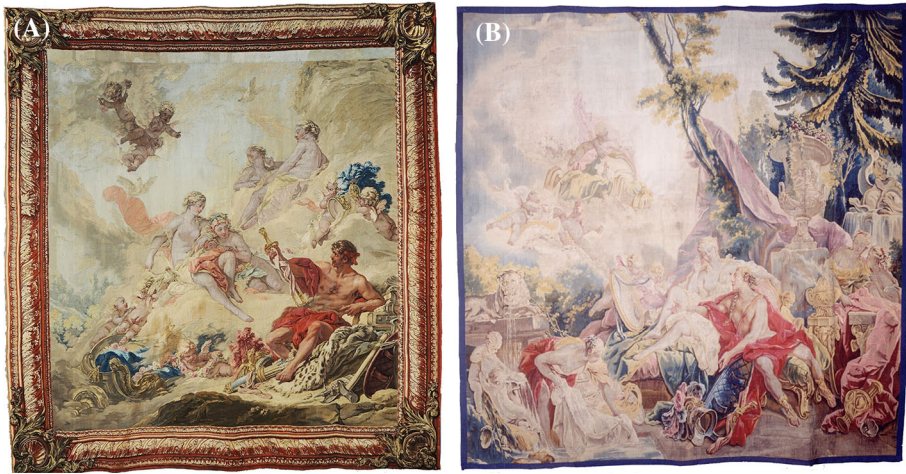


**Fig. 2** A «Amours des Dieux Venus et Vulcain» (GMTT-205-002) (3.25 m × 3.5 m) from a cartoon by F. Boucher, Gobelins Manufacture —1759. Photograph © Isabelle Bideau; B «Amours des Dieux Mars et Vénus» (GMTT-388-00) (3.21 m × 3.23 m) from a cartoon by F. Boucher, Beauvais Manufacture-1750—Photograph © Mobilier National

### 2.2.1 Aubusson manufacture

This Aubusson tapestry (Fig. 1) was woven in 1753 after a cartoon by Jean-Joseph Dumons, famous painter to the King in Aubusson Manufactory. Largely due to Dumon's paintings of great quality, the manufactory achieved great fame from 1731. This high-quality tapestry depicts a landscape, a speciality of Aubusson at that time, and belongs the category of “*Verdures fines*”. It also has the particularity of bearing the arms of Count Heinrich von Brühl, first minister of August III, King of Poland, which is a testament to the high quality and the prestige of this tapestry.

### 2.2.2 Gobelins and Beauvais manufactures

Both of the Gobelins and Beauvais tapestries were made after the cartoons of the same painter: François Boucher. He was a famous French painter of the eighteenth century who directed the Beauvais Manufactory from 1734 onwards alongside Jean-Baptiste Oudry. Following Oudry's death in 1755, he became inspector of the Royal Gobelins Manufactory until 1765. In his capacity as painter at the Royal Academy and his functions in the Manufactories, he painted many tapestry cartoons leading to the realisation of many *Grand Teint* tapestries.

The «*Amours des Dieux Venus et Vulcain*» tapestry (Fig. 2a), kept at the *Mobilier National* in Paris, was woven at the Gobelins Manufactory in 1759. This work represents Vulcan presenting a sword to Venus surrounded by three nymphs and is signed “F. Boucher, 1757” [20, 21].

The third tapestry (Fig. 2b) is also curated at the *Mobilier National*. It was woven at the Beauvais Manufactory and was similarly created from a cartoon by François Boucher [22]. This tapestry represents the love affair between the gods Venus and Mars and is dated 1750 [23].



### 3 Methods

#### 3.1 Hyperspectral imaging (HSI)

Hyperspectral imaging sensors collect image data in hundreds of narrow adjacent spectral bands simultaneously, giving a continuous reflectance spectrum for each pixel of the hyperspectral image. Data were recorded using a line scanner with the camera placed upon a 1.30-m-long rail. A Spectralon fluoropolymer (99% reflectance) was used to cover the entire field of view of the detector. Captured during the data acquisition, this served as a white reference object. A second acquisition with the shutter closed was also performed and used as a dark reference to quantify the detector electronic noise. Overall, these black and white references were used for flat-fielding and to convert the data to reflectance factors. The artworks were illuminated with two halogen lamps oriented at 45° from the sample. The analyses were performed at a working distance of 1.1 m under 2200 lx illumination, resulting in a total exposure dose of 55 lx.h for both cameras.

In this research, two complementary cameras, developed by SPECIM (Finland), were used.

The visible–near infrared (V-NIR) camera is a CCD camera (HS-XX-V10E) with a 2.8-nm spectral resolution (FWHM), a spectral sampling of 0.7 nm, and a pixel size of 54.7  $\mu\text{m}^2$ . This moving camera allows for the building of a data cube where the first two dimensions are spatial (1600 pixels  $\times$  X pixels) (with X corresponding to the number of pixels in the width of the image). The third dimension is a spectral dimension (840 bands). The wavelength range extends from 400 to 1000 nm.

The short-wave infrared (SWIR) camera is equipped with a cryogenically cooled mercury Cadmium telluride (MCT) detector with a 12-nm spectral resolution (FWHM), a spectral sampling of 5.6 nm, and a pixel size of 576  $\mu\text{m}^2$ . The dimensions of the data cube are 384 pixels  $\times$  X pixels  $\times$  288 spectral bands, with a spectral range of 1000–2500 nm.

Spectra acquisition, storage, and calibration were performed using IDAQ software. The data cube's creation and analysis were completed using ENVI 5.2 + IDL software. False colour images can be generated by assigning red, green, and blue colours to three different spectral bands in the ENVI software. A reflectance spectrum for each pixel can then be exported. In most of the reflectance spectra presented, the Y axis represents the reflectance factor, but the spectra were offset to ensure a better readability of the data. To create the external database, a reflectance spectrum for each sample of the colour chart was extracted by averaging the spectra of a window of 10 by 10 pixels (size: 547  $\mu\text{m}^2$ ). To ensure better results, the spectra of the data cube were cut from 1000 to 850 nm. This was necessary due to a bad signal: noise ratio and resulted in the consideration of only the best resolved data.

#### 3.2 Classification methods

Two methods of classification were used for analysis, the external or internal database. With the first method, a database of spectra is recorded from samples independent of the work. In our case, the colour chart of recreated eighteenth-century samples was used as a comparative database. These reference spectra were then compared with the spectra of the tapestry sample and mapped via SAM. The second method is to extract reference spectra directly from the item in question. In this analysis, these spectra were extracted through a series of steps using ENVI's Spectral Hourglass Wizard, the steps of which are explained in Sect. 3.2.2. Once these reference spectra were defined, the SAM application was also used to map the materials onto the work.

### 3.2.1 Spectral angle mapper (SAM)

This supervised classification method, the Spectral Angle Mapper, evaluates the angle between each spectrum at each pixel with the spectra of reference (endmembers) [24]. Reference spectra can be obtained from an external (colour chart created) database or internally (extracted from the image). Each spectrum is considered as an  $n$ -dimensional vector ( $n$  being the number of spectral bands), allowing the calculation of the angular difference  $\alpha$  between the associated spectrum and the reference vectors [25]. The maximum angle  $\alpha$  allowed is defined by the user, while smaller angles indicate greater similarity between the spectrum and the reference. This classification makes it possible to obtain maps of the dyes by associating a colour code with each “group” of spectra.

### 3.2.2 ENVI's spectral hourglass wizard (SHW)

First, the spectral data are reduced (minimum noise fraction (MNF) transforms) using two main component transforms to separate the noise from the data. Next, a search for the most spectrally pure pixels is performed via the Pixel Purity Index using 10,000 reflectance spectra with a threshold of 3 (it should be approximately two to three times the noise level) [26]. These pixels are then grouped and visualised to allow manual selection of endmembers. In this paper, the term endmember is used to name the reference spectra (spectra of pure materials) from the internal classification method. Those endmembers are created by averaging the pixels of the selected cluster in a 3-D-scatter-plot. Once these endmembers are extracted from the image, a SAM classification is performed. The tolerance angle  $\alpha$  between the endmember and spectra in the artwork is determined by averaging the spectra of each pixel assigned to that endmember. Once the average spectra of those pixels have the same spectral characteristic of the endmember compared, the angle  $\alpha$  is considered appropriate. In our analysis, the tolerance angle varied for each endmember (from 0.1 to 0.18 radians).

## 4 Results and discussion

For all of the results, the two classification techniques and the application methodologies were first compared and illustrated using the Aubusson tapestry as an example. In the end, the HSI in the SWIR turned out to be the most sufficient method to identify the fabrics. However, the V-NIR range was useful for probing the dyes. Subsequently, applying this methodology to the three tapestries allowed for a discussion on the comparison of the materials used in the eighteenth-century Royal Manufactories.

### 4.1 Textile identification

Hyperspectral imaging in the short-wave infrared range allowed us to obtain the spectral signature from the substrate, in this case the textile. According to eighteenth-century writings, *Grand Teint* tapestries were produced from only wool and silk. Although both wool and silk are proteinaceous materials, a difference in structure and the presence of sulphur-free amino acids in silk allows us to differentiate them [27]. Figure 3b shows the distribution of the two fabrics making up the Aubusson tapestry. The RGB channels have been fixed in the software on the signature bands of the silk [15, 28]: 2205 nm, 1575 nm, and 1536 nm ( $4531\text{ cm}^{-1}$ ,  $6349\text{ cm}^{-1}$ , and  $6510\text{ cm}^{-1}$ , respectively). The band at 2205 nm indicates the presence of protein  $\beta$ -sheet typical of the silk structure, while the bands at 1575 and 1536 nm are

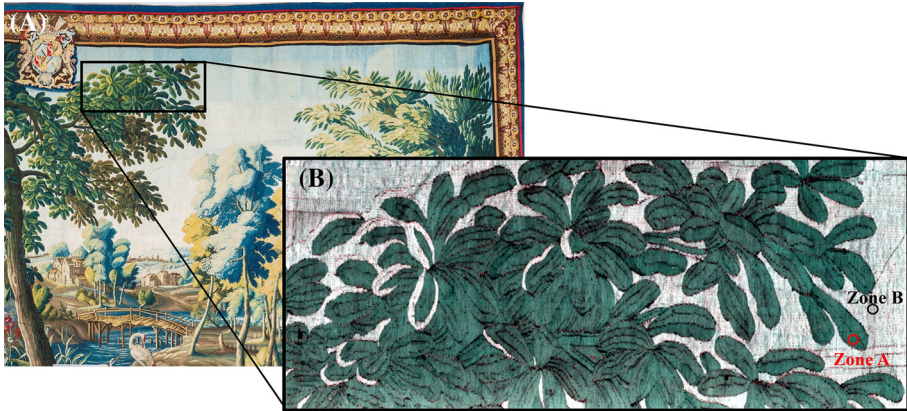


**Fig. 3** A Photographs of the top right corner of the Aubusson tapestry; black rectangle: analysed area of the tapestry (0.83 m  $\times$  0.3 m); B false colours hyperspectral image in the SWIR range ( $R = 2205$  nm;  $G = 1575$  nm;  $B = 1536$  nm)

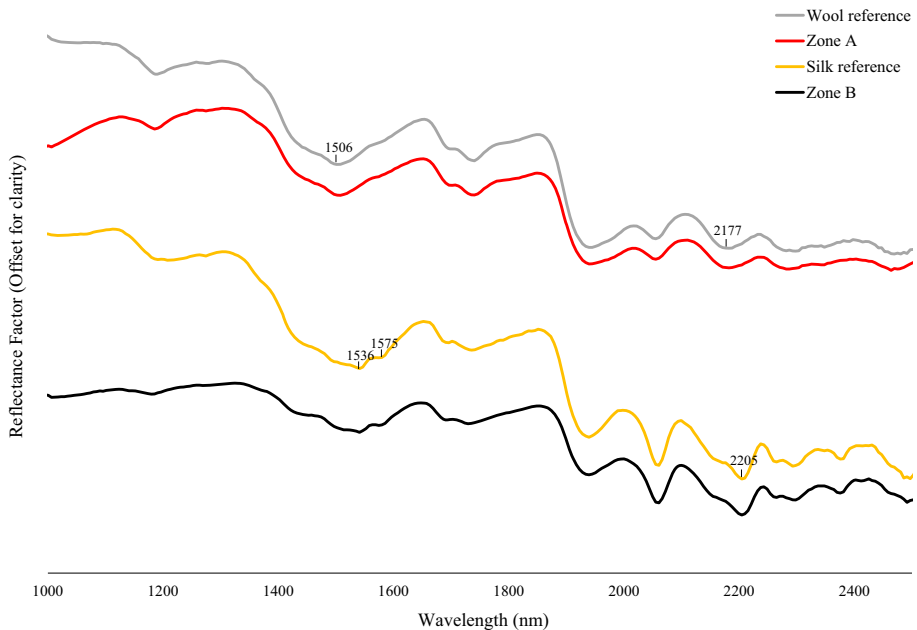


**Fig. 4** Grey and yellow lines: reflectance spectra of silk and wool references with their characteristic bands. Red and black: spectra of zones A and B from the Aubusson tapestry (respectively, red and black circles in Fig. 3B)

associated with the amide groups of the  $\beta$ -sheet. The significant bands of the wool occur at 2177 nm and 1506 nm and are associated with the  $\alpha$ -helical structure of the textile. In Fig. 3b, the areas made of wool appear green–blue, while the areas made of silk are white. Figure 4 shows typical reflectance spectra obtained in the SWIR range on a green–blue zone (Zone A, Fig. 3). They are compared with reference spectra where signature bands are pointed for silk and wool. This method thus appears to be effective in identifying and mapping textiles.



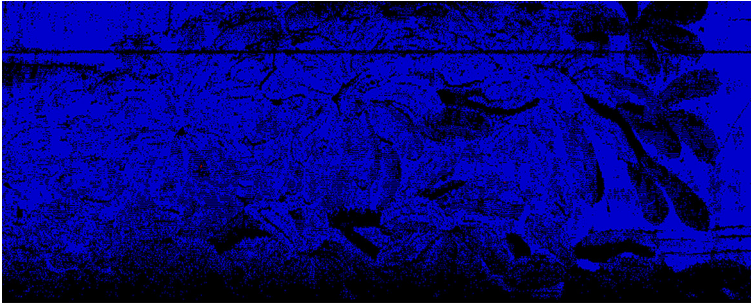


**Fig. 5** Classification performed with the SAM (maximum angle: 0.1) with our colour chart as a reference (analysed area: 0.83 m × 0.3 m)

In order to validate this approach based upon the mapping of the specific reflectance textile bands, two different tests were performed. First, the external database method with a SAM classification was performed. The external reference database was composed of one undyed wool sample and one undyed silk sample. The result obtained with an angle  $\alpha = 0.1$  radians of the SAM classification is displayed in Fig. 5. In this figure, the unclassified pixels are shown in black (*i.e.* the pixels where the SAM angle was outside of the chosen maximum angle). Blue pixels are associated with the reference corresponding to silk spectrum. When checking this result with the real spectra on the hyperspectral image and comparing it with Fig. 3b, it is observed that all of the wool areas were either attributed to silk or not attributed at all. Results with a slightly higher or lower  $\alpha$  value give a similar result. Indeed, when the angle is increased, all pixels end up being attributed to the silk reference. On the contrary, when  $\alpha$  is decreased, the pixels are no longer classified. In the end, despite the angle chosen, no pixel is ever attributed to the wool. This method therefore does not seem to be reliable for the identification of textiles given the constraints of our reference sample.

For comparison, a classification with extraction of the endmembers beforehand was performed and is displayed in Fig. 6. This treatment allowed the extraction of two reference endmembers from the image. The spectra of these endmembers, shown in Fig. 6b, exhibit the significant bands of silk for endmember #1 and wool for endmember #2. Furthermore, the results of the textile mapping correspond well to those obtained in Fig. 3b and thus allow for a very precise separation between wool and silk.

Of the two, the extraction of endmembers (*i.e.* internal database) appears to be a more reliable method. As our raw textile reference spectra are too different from those of the tapestry, it appears that the classification with an external database reference is not possible. The reasons for the difference between our reference material and the archaeological sample will be detailed later. However, these tests have shown that the technique of pointing at the vibrational features of the silk with the RGB channels is sufficient in mapping the textiles. This technique was applied to all of the areas analysed in the studied tapestries. Ultimately, observations matching the false colour hyperspectral images in the SWIR and photographs of the tapestries allowed a comparison of patterns of the textiles used in the Manufactories.

False colour images in the SWIR range allowed us to “map” the textiles on the Aubusson tapestry (Fig. 7a and b). This mapping revealed that the silk is only used for areas of lighter shades (beige, ivory and yellow), while the darker colours (blue, red or green) are dyed on wool. The silk is used sparingly and only on small areas or in the middle of a wool area to add dimension to the design. In the Aubusson Manufactory, the choice of the fabric used seems to be dictated by the colour which it had been dyed. In contrast, the Beauvais Manufactory

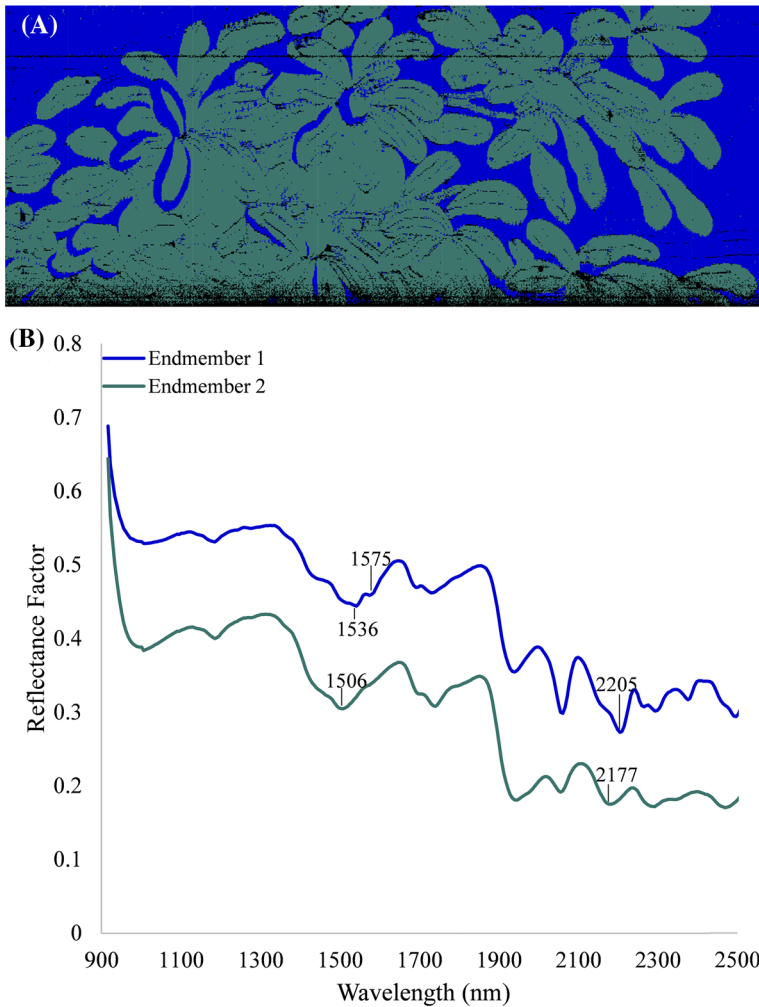


**Fig. 6** A Classification performed with the SAM (maximum angle: 0.1) after SHW and endmembers extractions. (MNF dimensionality: 15, PPI threshold value: 3, PPI number of iterations: 10.000) (analysed area: 0.83 m × 0.3 m); B reflectance spectra of the two extracted endmembers

seems to have used a different technique. This is apparent in Fig. 7c, which shows that the type of textile used was selected based upon design area without consideration of colour. To this point, the beige hair and the red or ivory dresses are made of silk, while the light flesh-coloured bodies and the dark blue-green bush in the background are woven from wool. Finally, the tapestry from the Gobelins Manufactory presents a textile distribution using the characteristics of the two other tapestries. Indeed, Fig. 7b shows that the textile is distributed without distinction of the colour used but rather according to the imagery of the drawing itself. In this example, the wool is used for the beige body skin or the red dress. Silk is therefore used in large areas but also in small zones such as in Vulcan's hair to symbolise the reflections, thus adding dimension as is similarly observed in the Aubusson tapestry. The

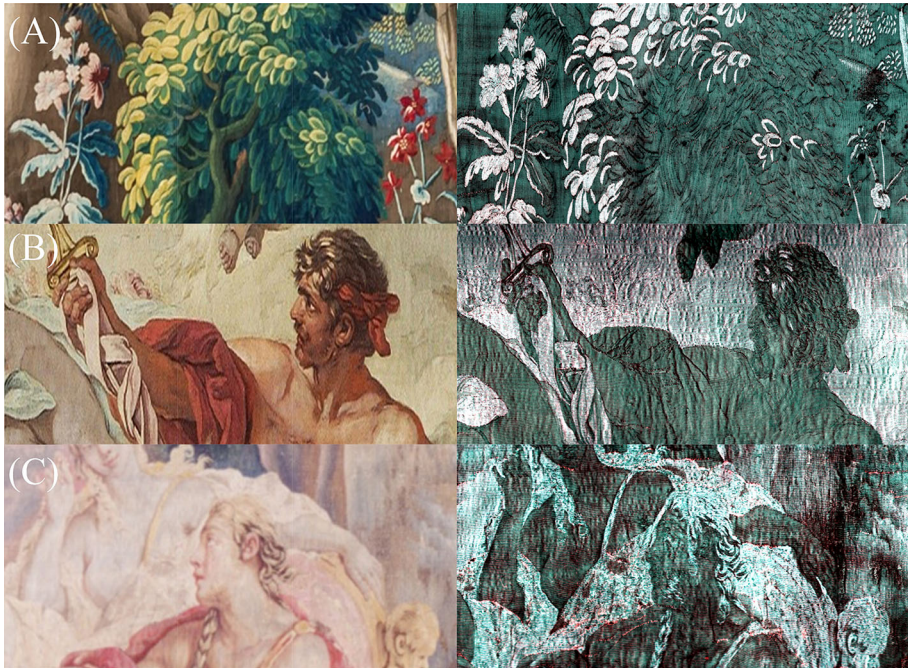


**Fig. 7** Left: photograph of an area of the tapestry; right: hyperspectral imaging false colours in the SWIR range ( $R = 2205$  nm;  $G = 1575$  nm;  $B = 1536$  nm). A Aubusson; B Gobelins; C Beauvais

observations made on these detail images shown in Fig. 7 can likewise be found for the entirety of each respective tapestry.

These technical and aesthetic choices may reflect an economic consideration by the Aubusson Manufactory. In this regard, they may have reduced the quantity of silk used, perhaps due to this fabric being more expensive than wool. Conversely, it could also highlight the greater prestige of the Gobelins and Beauvais Manufactories, whose tapestries contain large quantities of the more expensive silk.

#### 4.2 Dye identification through the example of madder colour chart

The reflectance spectra in the V-NIR range have proven to be more suitable for dye identification. Because several factors can influence the classification of tapestry materials, it is important that the treatment of the data be conscientious. Firstly, the state of conservation of the tapestry can have an impact on the identification of the materials. In our sample, the artwork has, in fact, been damaged in certain areas, and the layer of dust accumulated over time modifies the colour of the threads, particularly when colours are light. This phenomenon warrants the need to extract end members directly from the image, rather than using an external database. In addition, problems with differences in reflectance can be induced by the structure of the material itself. The tapestry is not a completely flat surface due to its conservation state and because it is woven with wool or silk threads. As these threads are curved, the light received during an analysis is not exactly identical between the top, the middle, and the bottom of the thread. This structure creates some differences in absorption between these zones and consequently between different pixels. Finally, a colour can be optically created

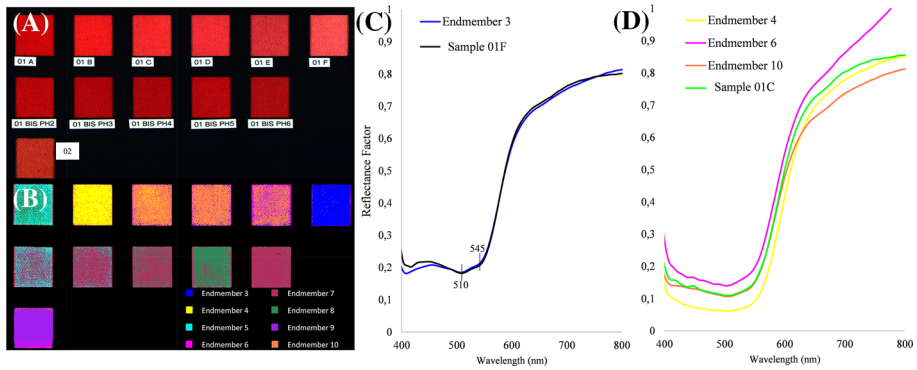


**Fig. 8** A Photographs of the madder colour chart, B classification SAM ( $\alpha = 0.2$ ) after SHW of the madder colour chart (endmembers 1 and 2 are linked to the black paper and labels and are therefore not shown in this representation) (MNF dimensionality: 23, PPI threshold value: 3, PPI number of iterations: 10.000), C endmember 3 and reflectance spectrum of sample 01F, D endmember 10 and reflectance spectra of samples 01C, 01D and 01E

by the interweaving of several threads of different colours. To account for this would require very fine spatial resolution and thus the search for dyes and their accurate identification can become quite complicated.

In order to assess these issues, a test of the internal database system via the ENVI-SHW was carried out on a colour chart of madder. From this colour chart (Fig. 8a), the endmembers were internally extracted with the SHW process. A SAM classification was then performed to associate the endmember with pixels of the colour chart (Fig. 8b), giving each endmember a defined colour.

Figure 8 shows that some endmembers are very well defined and can indeed map an area as is evidenced on sample 01F. In Fig. 8b, the classification shows that sample 01F is almost entirely (95%) associated with blue pixels (59,588 out of 63,200 pixels analysed are blue). Figure 8c shows the spectrum directly extracted from sample 01F (Fig. 8a) and endmember #3 associated with the blue pixels on the SAM classification (Fig. 8b). The two spectra are indeed very close and have the same characteristic absorption bands of madder at 510 and 545 nm [11]. Those absorption maxima are due to  $n \rightarrow \pi^*$  transitions of carbonyl groups present in the molecules of alizarin, of which madder is mainly composed [29]. The spectra also show a rather strong reflection band between 420 and 450 nm which has likewise been observed in other cases [30]. Figure 8b shows, on the other hand, that the assignment via the internal database is not always homogeneous even when the spectra are extracted from the object itself. For the same formulation, the processing associates up to three endmembers (e.g. sample 01C and 01E). Figure 8d illustrates the fact that when the spectrum does not contain any specific bands but only a broad absorption band and a difference in intensity, it is difficult to discriminate one area from the other. Indeed, sample 01C shows mostly a strong broad absorption band from 410 to 560 nm, thus masking the two specific bands of madder (510 and 545 nm), a phenomenon previously observed elsewhere [30, 31]. This is due to the higher madder concentration of this sample and to the colour being darker. Thus, sample 01C is associated with 4 different endmembers, with the majority of the pixels being attributed to endmember #10, similar to samples 01D and 01E. This can be problematic, especially for yellow dyes or tannins which have broad absorption bands but a different shade on the tapestry. Fortunately, other clues are present with some yellows dyes and can



assist in identification [32]. Moreover, this process identifies the zones differently according to the flatness of the surface which can cause erroneous attributions. As stated above, these problems are found on the tapestry as the weave is not completely flat. The selection of the correct  $\alpha$  is therefore very important because, when increased, it can avoid the problems related to the flatness of the sample. However, if it is too high, it risks associating pixels with close spectra but different shades.

#### 4.3 Identification of other dyes

For the purposes of identifying dyes, the internal method was applied on the tapestry. In doing so, a classification with the SAM algorithm (Fig. 9b) was performed after the extraction of 10 endmembers with ENVI-SHW. The endmembers were divided into three categories: green, yellow/brown, and red shades.

Figure 9c displays 4 endmembers whose corresponding pixel shades on the tapestry are green. It is known that green shades were composed of fabrics dyed initially with a base of blue, from either indigo or woad for the *Grand Teint* dyes [3]. In this case, spectra exhibit an absorption maximum at 660 nm and an inflection point at 720 nm, as a result of the presence of indigotin that is the main constituent of indigo and woad [11, 30]. Next, the blue textile is soaked in a yellow dye bath, the formulation and soaking time being determined by the shade desired. The list of *Grand Teint* yellow dyes was made up of weld, dyer's broom, safflower, fenugreek, and old fustic. The first four species are mainly composed of molecules such as luteolin or genistein belonging to the flavonoid family. This makes their absorption and therefore their reflectance spectrum very similar, with an absorption band between 400 and 460 nm depending on their shade. Old fustic, which is mainly composed of maclurin of the ketone family, also displays a broad band in the same spectral range [32]. Further, in the spectra of endmembers #3, #6, #7, and #8, the existence of a second absorption maximum at 415 nm confirms the presence of a yellow dye. This study therefore highlights the diversity of shades used in the tapestry as this relatively small area appears to be composed of at least four different greens.

Figure 9d shows the spectra of endmembers corresponding to yellow, white, or brown pixels. The spectrum of endmember #1 displays the typical relatively flat shape of a brown obtained from tannins of the polyphenol family. *Grand Teint* dyes authorized to dye tawny and brown included walnut stain, sumac, alder bark, and walnut root. Endmembers #5, #9, and #10 are examples of the problems specific to tapestries that can be caused by weaving and by the numerous shades used. First, in the area in the green square in Fig. 9a, only one shade of white is present. Yet, the distance between the threads creates a shadow and consequently darker pixels, thus creating a "fake" endmember, (*i.e.* #10). Indeed, the inauthenticity of this endmember is demonstrated in the green square in Fig. 9b. Here, the grey pixels assigned to endmember #10 are arranged in a line between the pixels assigned to endmember #5, thus indicating a shadow between threads. Spectra from the yellow pistil, white petal, and white leaf areas were also extracted for comparison with endmembers #5 and #9. Results suggest that, despite the appearance, the white area of the leaf is in fact a green. In this case, the degradation of the tapestry has turned this colour from a green to a very light yellow to white in terms of its appearance to the human eyes. Indeed, the spectrum (Fig. 9d) shows an absorption band at 660 nm, which is significant for indigotin and a maximum at 415 nm whose likely provenance is from flavonoids. The spectrum extracted from the white zones of petals also shows a maximum at 415 nm, while there is a maximum at 420 nm for the pistils. The latter two areas would have therefore originally been two different shades of yellow. Endmember #5 appears to be a mixture of spectra from the two white areas (leaf and petal),



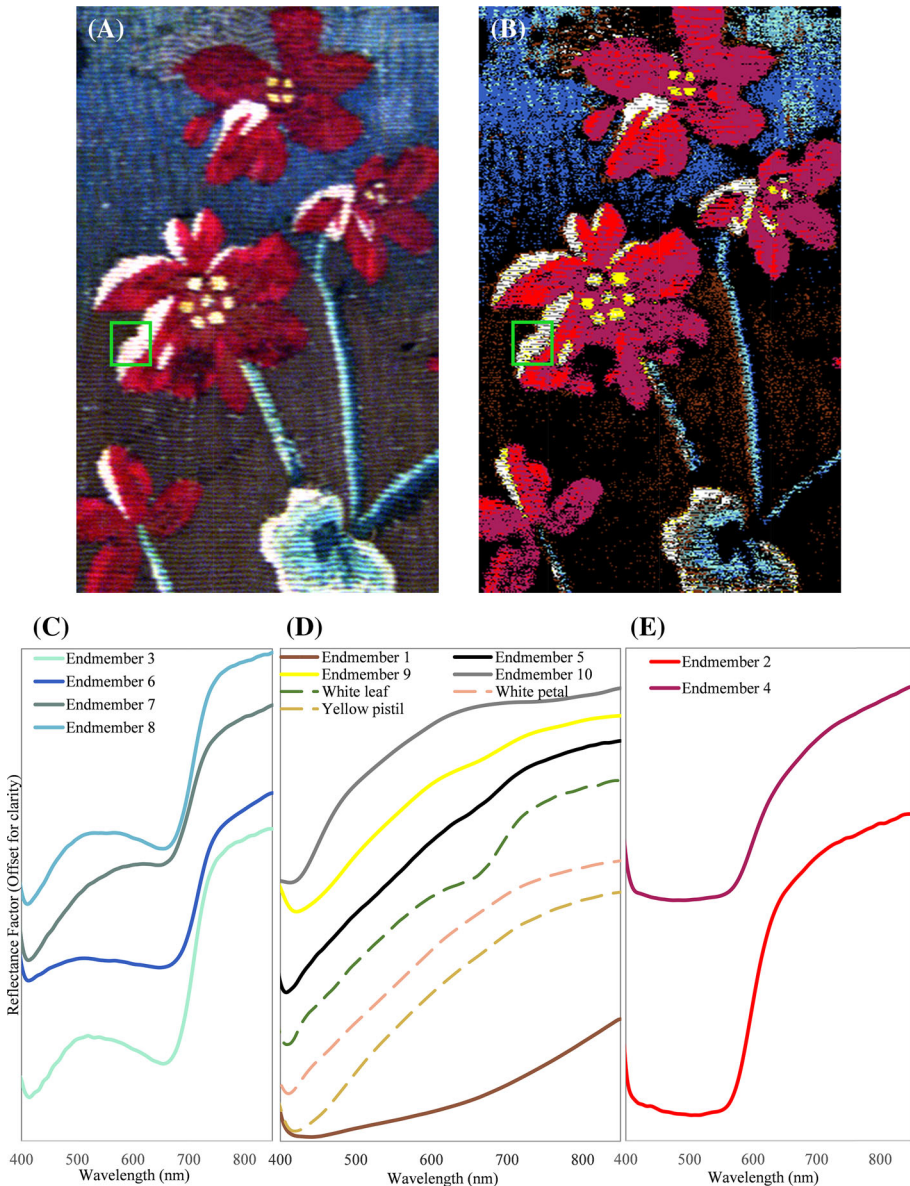


**Fig. 9** A Visible hyperspectral imaging ( $R$ : 650 nm;  $G$ : 540 nm;  $B$ : 450 nm) of a detail of the Aubusson tapestry ( $8,3 \times 24,8$  cm), B SAM classification after ENVI-SHW (MNF dimensionality: 12, PPI threshold value: 3, PPI number of iterations: 10.000, angle  $\alpha$ : 0.12–0.18 radians.); reflectance spectra of the endmembers extracted, C green, D yellow and brown, E red (pixels corresponding to endmember #5 (grey line) appears white on (B))

which is confirmed by the classification in Fig. 9b, where the white pixels of endmember #5 are found in both areas. In the case of very close shades, it is therefore critical to double-check the data directly on the hyperspectral image. This highlights one of the limitations of internal endmember extraction in this particular material.

Finally, Fig. 9e illustrates that spectra of endmembers #2 and #4 show a broad absorption band from 560 nm, indicating a high concentration of madder. In addition, spectrum #2 exhibits a very weak band at 515 nm, further confirming the use of this dye. The absence of the two specific bands (505–515 nm and 540–550 nm) [11, 30] on the spectrum of endmember #4 highlights the phenomenon already observed on the colour chart.

Figure 9b shows that some endmembers have not been extracted, such as the dark blue of the leaf centre or the almost-black red of the petals. This absence can sometimes be attributed to the pixels selection by the PPI algorithm. Clearly, if no pixels are selected in these areas, the clusters determining the endmembers will not contain the associated spectra. This phenomenon, although already observed elsewhere by Kleynhans [18], is not the origin of the problem in our case, however. Upon further inspection, one pixel in the blue area and two pixels in the dark red petal area were in fact found. Subsequently, after another observation of the 3-D-scatter-plot, these pixels were identified and the endmembers could be successfully extracted. It is worth noting that this seems to occur on the darkest, almost black colours. But this example nonetheless demonstrates the importance of a very thorough and accurate cluster selection.

Comparing the results from the three tapestries reveals an important similarity. Notably, they have the common characteristic of having a blue sky dyed with indigo on silk. Today, the skies in the tapestries appear to be almost white or grey to the naked eye, with a very light blue tint. In the Aubusson tapestry, the sky is the only place where indigo alone is used to dye the silk. In all the other areas, yellow is also used. On the other hand, indigo is used alone and as a mixture when dyeing wool. The Gobelins tapestry, by contrast, shows numerous areas of indigo dyed on silk (*e.g.* the quiver of arrows at Vulcan's foot (Fig. 2a)). Although the reflectance spectra do not differentiate between indigo and woad, ancient treatises instruct the dyer not to dye silk with the woad tank, as this plant does not dye this textile quickly enough [4]. This information leads to the hypothesis that all of these blues on silk were in fact dyed with indigo. It is also observed that all of the blues dyed upon silk are degraded and appear almost white today. These observations therefore raise the question of whether the Gobelins artists were aware of this phenomenon of degradation. If so, did they choose the luxury of silk to the detriment of the colour holding?

Another notable difference is the use of cochineal. Indeed, this red insect-based dye is more common at Gobelins and Beauvais, in comparison with the Aubusson Manufactory, which uses mainly madder. The Aubusson tapestry that displays the arms of Count von Brühl features only two very restricted zones (pink flowers) that used cochineal, both of which only use this dye to obtain a pink. All other shades from red to purple found on this tapestry are made of madder (mixed with another dye). The two other tapestries, however, feature numerous pinkish shades and use madder only for the red in Vulcan's robe (Fig. 2a) and that of Mars (Fig. 2b). All other shades of red were created through the use of cochineal.

Finally, the Aubusson tapestry seems to present an overall greater variety of shades. For example, green is expressed in at least five different shades in one area alone. However, given that the image themes presented are different, the variety of shades utilised may be due to aesthetic choices and/or because of the subject matter being portrayed. For a fuller understanding of the hyperspectral results, in the future it could also be beneficial to take a multi-analytical approach such as through the use of portable X-Ray Fluorescence (pXRF) [33–35] for mordants or microspectrofluorimetry [36, 37] for flavonoids [32]. Further, these

data may also be complemented, in some cases, with invasive methods that have been established for the identification of dyes, such as chromatography coupled with mass spectrometry [10, 38–40].

## 5 Conclusion

The analyses performed in this paper raised many observations concerning the use of materials in the three Royal Manufactories of tapestry during the eighteenth century. Indeed, the mapping from hyperspectral imaging, as opposed to point methods, allowed for the rapid visualisation of the dyes and textiles used as well as the identifying the correlation between textile use and colour. Both wool and silk were used for tapestry production, but were dyed in different ways. For example, textiles were dyed with madder and indigo on wool and weld or light colours on silk in Aubusson, whereas cochineal and indigo were dyed either on wool or silk at the Gobelins and Beauvais Manufactories. Our analyses also highlight the less frequent use of silk or cochineal in Aubusson.

HSI in V-NIR and SWIR proved to be effective methods for the identification and mapping of materials (dyes and fibres) of old tapestries. However, in the case of tapestries, there are certain complexities due to light degradation and the non-planarity of the surface. This paper shows the consequences of those material particularities on the classification methods. Indeed, the external method is less efficient due to the use of “fresh” (not degraded) samples with the colour chart. The classification methods with internal reference used through ENVI-SHW, on the other hand, provide a more effective first approach to identifying the distribution of textiles used in the SWIR range (as well as indicating the vibrational features via the RGB channels). This method also allows us to map the different dyes and to identify dyes with an easily recognisable spectra in the V-NIR range. In the future, this treatment should be further developed to facilitate the differentiation of areas where the same dye is used but in different shades. Presently, the effects of degradation and/or material geometry can cause misleading classifications due to the separation of pixels that have been dyed using the same formulation.

Finally, the power of hyperspectral imaging and its use in two domains (V-NIR and SWIR) has enabled many observations that may indicate a real economic difference between the different manufactories. Furthermore, the results indicate that sometimes the imagery, the richness of the theme, and/or the materials may have taken precedence over technical considerations. For example, one can wonder if the use of indigo, which fades quickly when used as a silk dye, is indicative of more than a simple desire to show the luxury of the Gobelins Manufactory as compared to others. Overall, given these results, this analysis thus allows for a better understanding of the place that the Aubusson Manufactory occupied within the French economic and artistic landscape.

**Acknowledgements** Thanks are due to Emmanuel Gérard, director, and Bruno Ythier, curator at the time of this study, and Alice Bernadec new curator of the *Cité Internationale de la Tapisserie* in Aubusson, who gave us access to the collection. We are also grateful of H  l  ne Gasnault, curator of *Mobilier National et Manufactures Nationales*, who authorised access to the collection. The authors would like to thank Charlotte Marembert, master dyer at the *Myrobolan workshop*, for creating the colour chart samples.

**Funding** This project has received support from the French State managed by the National Research Agency under the programme Future Investments bearing the reference ANR-10-LabX-52. The Conseil Regional Aquitaine also provided funding for this research with a grant numbered “2019-IRM0401”. This project also received a donation from a patron (Galerie Chevalier) as well as receiving financial support from the French government in the framework of the University of Bordeaux’s IdEx “Investments for the Future” program/GPR “Human Past”.

**Data availability** The data that support the findings of this study are available from the corresponding author upon reasonable request.

## Declarations

**Conflict of interest** The authors have no conflicts of interest to declare that are relevant to the content of this article.

## References

1. P. Bertrand, Aubusson, tapisseries des lumières: splendeurs de la manufacture royale, fournisseur de l'Europe au XVIII<sup>e</sup> siècle. Snoeck, Heule (2013)
2. C.-F.C. Du Fay, Observations physiques sur le mélange [sic] de quelques couleurs dans la teinture. In: *Histoire de l'Académie Royale des sciences avec les Mémoire de Mathématique & de Physique pour la même Année* (Imprimerie Royale, Paris, 1737), p. 253–268
3. J. Hellot, L'art de la teinture des laines et des étoffes de laine en grand et petit teint, avec une instruction sur les déboüillis. Paris (1750)
4. P.-J. Macquer, Art de la teinture en soie. Paris (1761)
5. C.-L. Berthollet, Éléments de l'art de la teinture. Paris (1791)
6. D. Cardon, Le monde des teintures naturelles. Belin (2003)
7. C. Viel, Colorants naturels et teintures du XVII<sup>e</sup> siècle à la naissance des colorants de synthèse. *Pharm* **93**, 327–348 (2005). <https://doi.org/10.3406/pharm.2005.5848>
8. D. Diderot, J. L. R d'Alembert, *L'Encyclopédie, ou Dictionnaire Raisonné Des Sciences, Des Arts et Des Métiers*. 306–315. Paris (1751)
9. D. Tamburini, J. Dyer, Fibre optic reflectance spectroscopy and multispectral imaging for the non-invasive investigation of Asian colourants in Chinese textiles from Dunhuang (7th–10th century AD). *Dyes Pigm.* **162**, 494–511 (2019). <https://doi.org/10.1016/j.dyepig.2018.10.054>
10. J. Dyer, D. Tamburini, E.R. O'Connell, A. Harrison, A multispectral imaging approach integrated into the study of Late Antique textiles from Egypt. *PLoS ONE* **13**, e0204699 (2018). <https://doi.org/10.1371/journal.pone.0204699>
11. M. Aceto, A. Agostino, G. Fenoglio, A. Idone, M. Gulmini, M. Picollo, P. Ricciardi, J.K. Delaney, Characterisation of colourants on illuminated manuscripts by portable fibre optic UV-visible-NIR reflectance spectrophotometry. *Anal. Methods* **6**, 1488 (2014). <https://doi.org/10.1039/c3ay41904e>
12. L. de Viguier, N.O. Pladevall, H. Lotz, V. Freni, N. Fauquet, M. Mestre, P. Walter, M. Verdager, Mapping pigments and binders in 15th century Gothic works of art using a combination of visible and near infrared hyperspectral imaging. *Microchem. J.* **155**, 104674 (2020). <https://doi.org/10.1016/j.microc.2020.104674>
13. J.K. Delaney, J.G. Zeibel, M. Thoury, R. Littleton, M. Palmer, K.M. Morales, E.R. de la Rie, A. Hoenigswald, Visible and infrared imaging spectroscopy of Picasso's *Harlequin Musician*: mapping and identification of artist materials *in Situ*. *Appl. Spectrosc.* **64**, 584–594 (2010). <https://doi.org/10.1366/000370210791414443>
14. C. Cucci, J.K. Delaney, M. Picollo, Reflectance hyperspectral imaging for investigation of works of art: old master paintings and illuminated manuscripts. *Acc. Chem. Res.* **49**(10), 2070 (2016)
15. J.K. Delaney, P. Ricciardi, L. Glinsman, Use of near infrared reflectance imaging spectroscopy to map wool and silk fibres in historic tapestries. *Anal. Methods* **8**, 7886–7890 (2016). <https://doi.org/10.1039/C6AY02066F>
16. A. Mounier, G. Le Bourdon, C. Aupetit, C. Belin, L. Servant, S. Lazare, Y. Lefrais, F. Daniel, Hyperspectral imaging, spectrofluorimetry, FORS and XRF for the non-invasive study of medieval miniatures materials. *Herit. Sci.* **2**, 24 (2014). <https://doi.org/10.1186/s40494-014-0024-z>
17. F. Daniel, A. Mounier, J. Pérez-Arantegui, C. Pardos, N. Prieto-Taboada, S. Fdez-Ortiz de Vallejuelo, K. Castro, Hyperspectral imaging applied to the analysis of Goya paintings in the Museum of Zaragoza Spain. *Microchem. J.* **126**, 113–120 (2016). <https://doi.org/10.1016/j.microc.2015.11.044>
18. T. Kleynhans, D.W. Messinger, J.K. Delaney, Towards automatic classification of diffuse reflectance image cubes from paintings collected with hyperspectral cameras. *Microchem. J.* **157**, 104934 (2020). <https://doi.org/10.1016/j.microc.2020.104934>
19. M. Delormois, *Le teinturier parfait*. Paris (1716)

20. M. Fenaille, F. Calmettes, État général des tapisseries de la manufacture des Gobelins depuis son origine jusqu'à nos jours, 1600–1900. Tome IV/publié par M. Maurice Fenaille (1903)
21. TAPISSERIE DE LICE – Amours des Dieux Vénus et Vulcain, <https://collection.mobilernational.culture.gouv.fr/objet/GMTT-205-002>
22. TAPISSERIE DE LICE – Les Amours des Dieux Mars et Venus, <https://collection.mobilernational.culture.gouv.fr/objet/GMTT-388-000>
23. E.A. Standen, The « Amours des Dieux »: A Series of Beauvais Tapestries after Boucher (1985)
24. Spectral Angle Mapper, <https://www.13harrisgeospatial.com/docs/SpectralAngleMapper.html>
25. F.A.F.A. Kruse, A.B. Lefkoff, J.W. Boardman, K.B. Heidebrecht, A.T. Shapiro, P.J. Barloon, A.F.H. Goetz, The spectral image processing system (SIPS)-interactive visualization and analysis of imaging spectrometer data. *Remote Sens. Environ.* **44**, 145–163 (1993)
26. Pixel Purity Index, <https://www.13harrisgeospatial.com/docs/PixelPurityIndex.html>
27. K. Mahall, *Quality Assessment of Textiles* (Springer, Berlin Heidelberg, Berlin, Heidelberg, 2003)
28. J. Workman, L. Weyer, *Practical Guide and Spectral Atlas for Interpretive Near-Infrared Spectroscopy* (CRC Press, London, 2012)
29. L. de Ferri, R. Tripodi, A. Martignon, E.S. Ferrari, A.C. Lagrutta-Diaz, D. Vallotto, G. Pojana, Non-invasive study of natural dyes on historical textiles from the collection of Michelangelo Guggenheim. *Spectrochim. Acta Part A Mol. Biomol. Spectrosc.* **204**, 548–567 (2018). <https://doi.org/10.1016/j.saa.2018.06.026>
30. M. Gulmini, A. Idone, E. Diana, D. Gastaldi, D. Vaudan, M. Aceto, Identification of dyestuffs in historical textiles: strong and weak points of a non-invasive approach. *Dyes Pigm.* **98**, 136–145 (2013). <https://doi.org/10.1016/j.dyepig.2013.02.010>
31. T. Vitorino, A. Casini, C. Cucci, M.J. Melo, M. Picollo, L. Stefani, Hyper-spectral acquisition on historically accurate reconstructions of red organic lakes (2014)
32. H. de Lacodre, C. Marembert, P. Claisse, F. Daniel, R. Chapoulie, L. Servant, A. Mounier, Non-invasive characterization of yellow dyes in tapestries of the 18th century: influence of composition on degradation. *Color Res. Appl.* (2021). <https://doi.org/10.1002/col.22646>
33. M. Radepont, J.-P. Échard, M. Ockermüller, H. de la Codre, O. Belhadji, Revealing lost 16th-century royal emblems on two Andrea Amati's violins using XRF scanning. *Herit. Sci.* **8**, 112 (2020). <https://doi.org/10.1186/s40494-020-00460-6>
34. Z. Szökefalvi-Nagy, I. Demeter, A. Kocsonya, I. Kovács, Non-destructive XRF analysis of paintings. *Nucl. Instrum. Methods Phys. Res. Sect. B* **226**, 53–59 (2004). <https://doi.org/10.1016/j.nimb.2004.03.074>
35. A. Kriznar, M. del Valme Muñoz, M.Á. Respaldiza, M. Vega, Materials applied in Bernardo Martorells painting analysed by portable XRF. *Archeosciences* **36**, 37–46 (2012)
36. G. Verri, C. Clementi, D. Comelli, S. Cather, F. Piqué, Correction of ultraviolet-induced fluorescence spectra for the examination of polychromy. *Appl Spectrosc.* **62**, 1295–1302 (2008). <https://doi.org/10.1366/000370208786822296>
37. M.J. Melo, A. Claro, Bright light: microspectrofluorimetry for the characterization of lake pigments and dyes in works of Art. *Acc. Chem. Res.* **43**, 857–866 (2010). <https://doi.org/10.1021/ar9001894>
38. I. Degano, E. Ribechini, F. Modugno, M.P. Colombini, Analytical methods for the characterization of organic dyes in artworks and in historical textiles. *Appl. Spectrosc. Rev.* **44**, 363–410 (2009). <https://doi.org/10.1080/05704920902937876>
39. E. Ferreira, A. Quyes, A.N. Hulme, H. McNab, LC-Ion Trap MS and PDA-HPLC- Complementary techniques in the analysis of flavonoid dyes in Historical textiles: the case study of an 18th century Herald's Tabard. *Présenté à Dyes in History and archaeology* (2003)
40. F. Pozzi, G. Poldi, S. Bruni, E. De Luca, V. Guglielmi, Multi-technique characterization of dyes in ancient Kaitag textiles from Caucasus. *Archaeol. Anthropol. Sci.* **4**, 185–197 (2012). <https://doi.org/10.1007/s12520-012-0092-5>